

Multi-lens, Multi-camera Calibration of Sony Alpha NEX 5 Digital Cameras

M. R. Shortis

School of Mathematical and Geospatial Sciences
RMIT University, GPO Box 2476 Melbourne 3001, Australia
mark.shortis@rmit.edu.au

Abstract

This paper describes close-range calibrations of multiple Sony Alpha NEX 5 consumer digital cameras with multiple interchangeable lenses. The standard physical parameter set and a standard parameter set with affinity and orthogonality terms are tested with both block-invariant and photo-invariant principal point parameters. The impact of the parameter sets is analysed to determine the effectiveness of the inclusion of these parameters in reducing systematic errors. The parameters are analysed to determine if a lens effect or camera effect is being modelled. Some conclusions are drawn regarding the possible physical sources of the systematic errors.

Key words: photogrammetry, close-range, calibration, parameters, multi-camera, multi-lens, stability

Author Biography

Mark Shortis is Professor of Measurement Science in the School of Mathematical and Geospatial Sciences and Director, Program Quality in the College of Science, Engineering and Health at RMIT University in Melbourne, Australia. Since the early 1980s he has been active in research in photogrammetry at close range, for example collaborative research with NASA Langley Research Center on the structural dynamics of aerospace models, with the University of Western Australia on underwater assessment of marine fish populations and habitats, with DLR Germany on the characterisation of solar concentrators for energy generation and with CSIRO Marine Research on deep water seabed mapping.

Introduction

To determine accurate measurements using close range photogrammetry, cameras must be calibrated. The parameters and techniques used for the calibration of cameras at close range are well established (Brown, 1971; Fryer, 1996, Fraser, 1997; Remondino and Fraser, 2006). Self-calibration using a calibration fixture or the measurement object is the accepted technique for the modelling and elimination of the systematic errors which would otherwise adversely affect the accuracy of the photogrammetric measurements (Kenefick et al., 1972). The details of the photogrammetric network solution based on collinearity and an iterative, least squares estimation solution are described in Granshaw (1980). In order to confidently derive the calibration parameters, the geometry of the photogrammetric network should be multiple, convergent photographs of a three dimensional target array or calibration fixture, preferably with a range of camera to object distances and a variety of orthogonal roll (rotation about the camera axis) angles to reduce correlations between parameters (Kenefick et al., 1972).

Previous camera calibrations, particularly in the field of high accuracy metrology, have demonstrated that camera calibration parameters can compensate for distortion effects that have no readily associated physical meaning. A typical example is the continued use and statistical significance of the image affinity term with the standard physical parameter model for camera calibration of both close-range (Reulke, 2006) and aerial (Cramer, 2004) digital cameras. This parameter was designed to compensate for affine film shrinkage, yet the parameter is still used regularly in calibration models for cameras with digital image sensors. An orthogonality term is also used in parameter sets to account for non-orthogonality of the x-y image coordinates, also known as image shear. Orthogonality is perhaps less frequently used and is only rarely reported as a significant term in the calibration set. Nevertheless, even though the physical effect of image shear is associated with photographic film, not with CCD and CMOS image sensors, the term is included in the '10 parameter' calibration set (Fraser, 1997). Both parameters are included in many close-range photogrammetry network adjustment software applications, for example Australis¹ and AICON 3D Studio².

¹ www.photometrix.com.au

² www.aicon.de

Calibration Parameters

Camera calibration at close-range is most often based on a set of physical parameters comprising the principal distance (PD), principal point (PP) location, radial and decentring lens distortions (Fraser, 1997). The primary physical parameters of the calibration define the location of the lens perspective centre with respect to the image sensor and the lens distortions that represent the departures from a perfect central projection. Radial and decentring lens distortion characteristics have been well established through extensive testing and validation over several decades since the initial formulation of the models (Brown, 1966; Ziemann and El-Hakim, 1983). One recent review has suggested that this physical parameter set is sufficient and extra parameters are not necessary for digital cameras (Remondino and Fraser, 2006). This contention is supported by calibrations that include these parameters but the analysis indicates that affinity and orthogonality are not significant (Chikatsu and Takahashi, 2009; Wendt and Dold, 2005), even when used with large area image sensor arrays (Mills et al., 2003; Rieke-Zapp, 2010).

A review of physical, empirical and combinations of types of additional parameters to model the secondary image non-linearities and image plane unflatness is given in Faig and Shih (1988). However because of the geometric regularity and stability of the sensor combined with digital transmission of the pixel data (Shortis and Beyer, 1996), modern CCD and CMOS sensors should not be subject to the classic image deformations associated with film or glass plate cameras (Fraser, 1997). Nevertheless both Fraser et al. (1995) and Shortis et al. (1995) found that the affinity term in the camera calibration parameter set was highly significant. Fraser et al. (1995) reports that the affinity term is strongly correlated with lenses, rather than cameras, in a calibration test that compared three different focal length lenses interchanged between two different resolution digital cameras. This suggests that the affine change in scale is associated with an optical effect rather than an image deformation. In contrast, Shortis et al. (1995) reports that the affinity terms is strongly correlated with cameras, rather than lenses, for two different scientific CCD cameras with two interchangeable lenses with different nominal focal lengths. This suggests that the affinity term is compensating for a physical property of, in that case, large format area array image sensors.

One confounding factor associated with consumer quality digital cameras is the lack of stability of the camera body, the image sensor mounting and the camera lens (Shortis et al., 1998; Rieke-Zapp et al., 2009). The poor reliability contributes systematic errors to the camera calibration and the effects may be partially compensated by parameters such as affinity and orthogonality.

The instability of the principal point location, caused by movement of the image sensor and the camera lens during manual handling, can be compensated using a photo-invariant model for the principal point (Mills et al., 2003; Moniwa, 1981; Shortis et al., 1998). This approach associates a unique principal point location with every photograph in the calibration network. The extra unknown terms in the least squares estimation solution tend to weaken the network, however the impact can be lessened if the network has a strong geometry and approaches hyper-redundancy by using many photographs and many targets (Fraser et al., 2005).

Experiment

Cameras

An opportunity arose to test the associations between calibration parameters for a ‘semi-professional’ or ‘prosumer’ compact digital camera. The opportunity was generated from the requirement to conduct a multi-camera, multi-lens calibration of three Sony Alpha NEX 5 digital cameras (see Figure 1) acquired by the University of Queensland. The cameras are deployed on an unmanned airborne vehicle (UAV) to capture multi-spectral imagery over mine closure sites, in order to monitor the potential impacts of underground mining (Lechner et al., 2012; Stecha et al., 2012).

The Sony NEX 5 cameras were chosen specifically because of the ability to interchange fixed focal length lenses, as well as the compact format, the high resolution, large area image sensor, the very light weight and relatively modest cost. The cameras currently have available Sony 16mm ‘pancake’ lenses and in the future LEICA 35mm and 50mm lenses will be acquired. The option of different fixed focal length lenses was a critical factor in the selection of the camera, because of the instabilities associated with zoom lenses (Shortis et al., 2006) which would otherwise add to the inherent instability of the body (Rieke-Zapp et al., 2009) for this class of prosumer camera.

The NEX 5 has a maximum image resolution of 4592 by 3056 pixels. The CMOS sensor is the APS-C format of 23.6 mm by 15.7 mm with a pixel spacing of 5.1 micrometres. Still images are recorded in JPEG format. The camera can also record HDTV format video, which is useful for the aerial imagery but requires a separate calibration (Shortis, 2011).

Two of the NEX 5 cameras have an unaltered image sensor. The image sensor has the standard visible spectrum cut filter that prevents the non-visible ultra violet and infra-red radiation reaching the CMOS array. These two cameras are designated RGB1 and RGB2. The third camera has been altered to enable infra-red sensitivity, because the near infra-red is important to landscape and vegetation studies. In this case the visible spectrum cut filter has been removed so that the camera becomes a 'full spectrum imager', sensitive to less than 350nm in the ultra violet and up to a wavelength of around 1000nm in the infra-red. For the mine rehabilitation application, an infra-red cut filter is fitted to the camera lens to block frequencies of less than 720nm. This camera is designated as NIR.

After the removal of the visible light filter, the back focus of the camera must be corrected because the refraction characteristics of the lens are altered by the change in the dominant wavelengths of light. Infra-red light is refracted less than visible light, so the plane of best focus is displaced away from the lens. This adjustment is made using shims or spring loaded screws, depending on the type of image sensor mounting.



Figure 1. Sony Alpha NEX 5 digital camera with the 16mm lens (www.sony.com)

Calibration

The three cameras must be pre-calibrated because a rigorous self-calibration is not feasible for the blocks of imagery routinely used for the landscape monitoring. The pre-calibration information is provided as input into the aero-triangulation software INPHO³, used to adjust the blocks of photography captured from the UAV. The cameras must be focussed at infinity for the pre-calibration, and it is essential that there are no unexpected correlations between calibration parameters that may introduce systematic errors and therefore produce perturbed values for the calibration parameters.

Accordingly, the calibration test range adopted for the pre-calibration must meet several requirements. First, the test range must be quite versatile to accommodate the different lenses and associated fields of view. To ensure high fidelity of the calibration parameters, especially the lens distortions, it is very important to ensure that the full format

³ www.inpho.de

of the sensor is covered by target images. Second, a large space is required to ensure infinity focus can be used and simultaneously retain all targets within the depth of field. Third, the test range must permit strong network geometry to minimise parameter correlations (Kenefick et al., 1972). Finally, the test range must be permanently established to allow for repeated calibration of the cameras to ensure the accuracy and reliability of the information derived from the aerial imagery.

An ideal test range is provided by the atrium of one of the buildings on the University of Queensland campus (see Figure 2). The approximate dimensions of the space are 10m by 20m by 12m, with three levels of usable volume to place targets and four levels to position camera stations. The ground floor is deemed unsuitable for targets because of the prominent impact on the aesthetics of the building and the potential for interference with the targets in the high pedestrian traffic areas. The space is flexible enough for all three lens types because the long galleries allow the range between the cameras and the targets to be varied to ensure that the target images fill the field of view of the cameras. Approximate coordinates of the targets were determined to a precision of $\pm 5\text{mm}$ using a total station.

Nine sets of calibration images were captured. Each calibration set comprised 24 exposures of the array of 62 targets from six camera stations. The cameras were rolled into four different orthogonal orientations at each camera station. The targets span approximately 6m by 12m by 8m in width, length and height respectively. The camera stations span an area of 5m width by almost 10m of height. The average camera to target horizontal separation is approximately 9m.

Each of the nine camera and lens combinations were initially processed in separate self-calibrating, internally constrained networks to determine initial calibration parameters and filter out any gross errors in the image measurements. The network adjustments were carried out using VMS⁴, which uses the standard physical model for calibration parameters with the option of block-invariant or photo-invariant principal point parameters (Shortis et al., 1998). The initial calibration model comprised only the primary physical parameters of block-invariant principal point location, principal distance and lens distortions. Target coordinates were used as starting values only and were subject to adjustment by the free network solution.

⁴ www.geomsoft.com



Figure 2. Calibration test range: target array (left), camera stations (right).

Inspection of the networks revealed that whilst some gross errors are readily attributed to problems such as partial occlusions, there is no apparent reason for a significant number of rejected image measurements near the edges of the camera format. The likely source of these rejections is the unusual radial distortion profile of the Sony 16mm lens and, in particular, the steep gradient at the edge of the field of view (see Figure 3). The gradient effectively magnifies image space errors and incorrectly classifies acceptable measurements as gross errors. In most cases these image measurements are retained in the data sets. To take advantage of hyper-redundancy (Fraser et al., 2005), the nine combinations of camera and lens were combined into one large, self-calibrating network. This network is used for the analysis of the different calibration models. The full network has more than 12000 redundancies and the average target is imaged on 106 exposures. There are just over 100 image measurements rejected by the outlier detection, with a high percentage of these near the edge of the format. Again the likely source of the concentration of rejections is the steep gradient of the radial distortion profiles.

Results and Analysis

A summary of the results of the self-calibrating network adjustments with the nine combinations of camera and lens is given in Table 1. Shown in the table is the RMS image residual, a prime indicator of the effectiveness of the calibration model used, and the mean precision of the target coordinates to indicate the object space precision. The table indicates clearly that a change in calibration model from block-invariant principal point to a photo-invariant principal point has a profound impact on the network, reducing the RMS image residual by half. In contrast, the inclusion of the image orthogonality and affine scale parameters has only a minor impact on the block-invariant model and no apparent improvement for the photo-invariant case.

Calibration Model	RMS Image Residual (um)	Mean Precision of Target Coordinates (mm)
Physical parameters only, block-invariant PP	1.24	0.55
Physical parameters only, photo-invariant PP	0.63	0.35
Physical parameters and affinity, orthogonality, block-invariant PP	1.21	0.53
Physical parameters and affinity, orthogonality, photo-invariant PP	0.63	0.35

Table 1. Results of the self-calibrating network adjustments with different calibration models.

Accordingly, the following results are based on the calibration model comprising physical parameters, affinity, orthogonality and photo-invariant principal point. In all cases the values of the parameters are significant at a 95% confidence limit.

Table 2 shows the mean principal point location in X and Y, and the principal distance for the nine combinations of camera and lens. The principal point location is defined as the intersection of the optical axis of the lens with the focal plane of the camera, so it would be expected that the X-Y coordinates would tend to follow the camera body. In Table 2 there is no obvious trend for the X coordinate of the principal point, which might suggest that the optical axes of the lenses are also playing a role in the variability. The Y coordinate of the principal point has a stronger association with the cameras than with the lenses, as indicated by the row and column standard deviations in Table 2. However there remains a significant level of variability, confirming that the principal point location is influenced by both the position of the sensor in the camera body and the location of the optical axis of the lens with respect to the lens mount. It is remarkable that Fraser et al. (1995) reports a very similar outcome in that the Y coordinate of the principal point was substantially more consistent than the X coordinate.

The unadjusted principal distances shown in Table 2 demonstrate a clear trend. The values for the two visible light sensitive cameras, RGB1 and RGB2, indicate that the principal distance is associated with the lens, as would be expected. The values for the NIR camera are consistently larger, by an average of 50 micrometres, reflecting the requirement to physically adjust the back focus of this camera for the infra-red sensitivity. Mills et al. (2003) reports a similar result for the removal of an infra-red cut filter. Once the NIR camera data is adjusted for this change, the values of the principal distances for each lens are consistent to 1-2 micrometres.

Principal Point X (mm)

Lens	Camera			SD
	RGB1	RGB2	NIR	
1	-0.346	-0.216	-0.226	0.072
2	-0.237	-0.090	-0.115	0.079
3	-0.236	-0.086	-0.081	0.088
SD	0.063	0.074	0.076	

Principal Point Y (mm)

Lens	Camera			SD
	RGB1	RGB2	NIR	
1	0.368	0.187	0.104	0.135
2	0.372	0.184	0.084	0.146
3	0.434	0.244	0.137	0.150
SD	0.037	0.034	0.027	

Principal Distance (mm)

Lens	Camera			SD	NIR Adjusted	SD
	RGB1	RGB2	NIR			
1	15.831	15.830	15.879	0.028	15.829	0.001
2	15.876	15.878	15.926	0.028	15.876	0.001
3	15.852	15.851	15.904	0.030	15.854	0.002
SD	0.023	0.024	0.023		0.023	

Table 2. Comparison of Principal Point location and Principal Distance for the nine combinations of camera and lens. SD = standard deviation.

The radial and decentring lens distortion profiles for the nine combinations of the three cameras and the three lenses are shown in Figures 3 and 4 respectively. It would be expected that the lens distortion profiles, both radial and decentring, would be consistent for each lens. This was unequivocally confirmed by both Fraser et al. (1995) and Shortis et al. (1995), reporting insignificant differences in lens distortion profiles at a 95% confidence limit. For the Sony 16mm lens there is some clustering of the distortion profiles evident for the lenses, especially for the decentring distortion of lens 2.

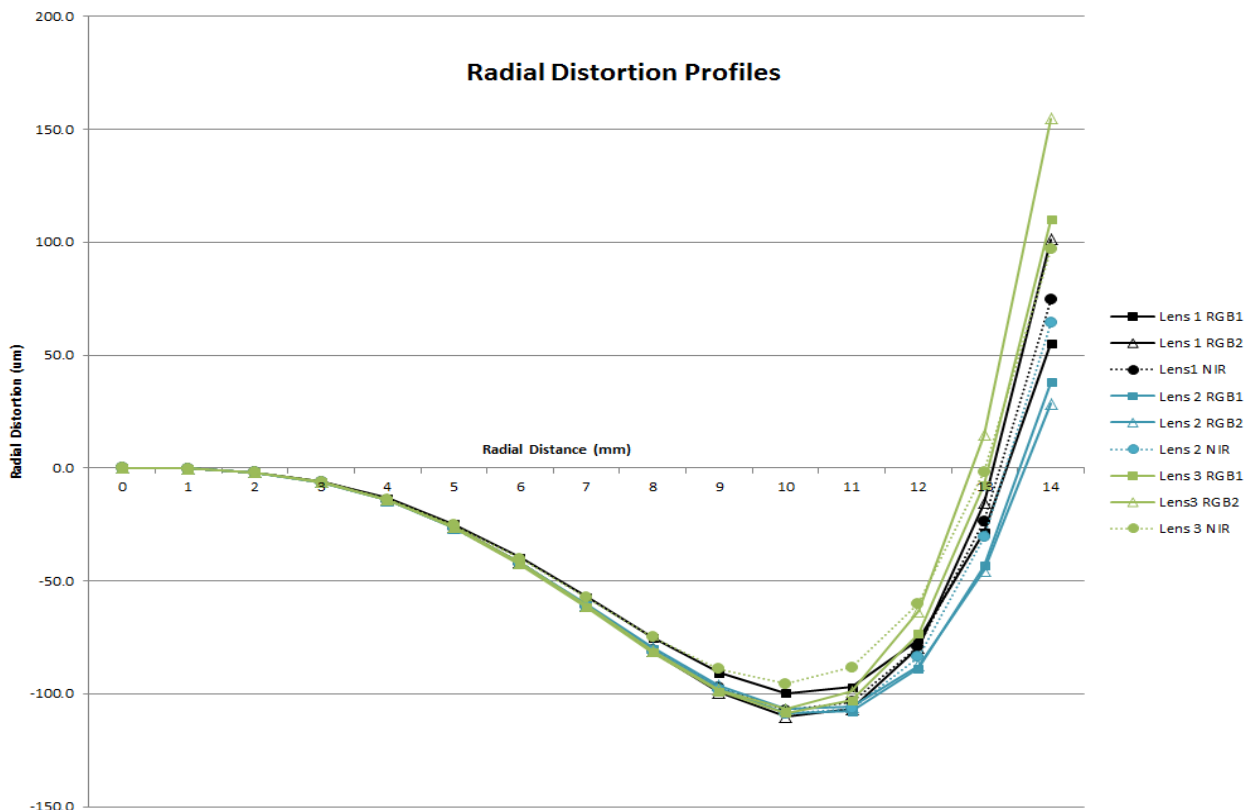


Figure 3. Radial distortion profiles for the nine combinations of camera and lens.

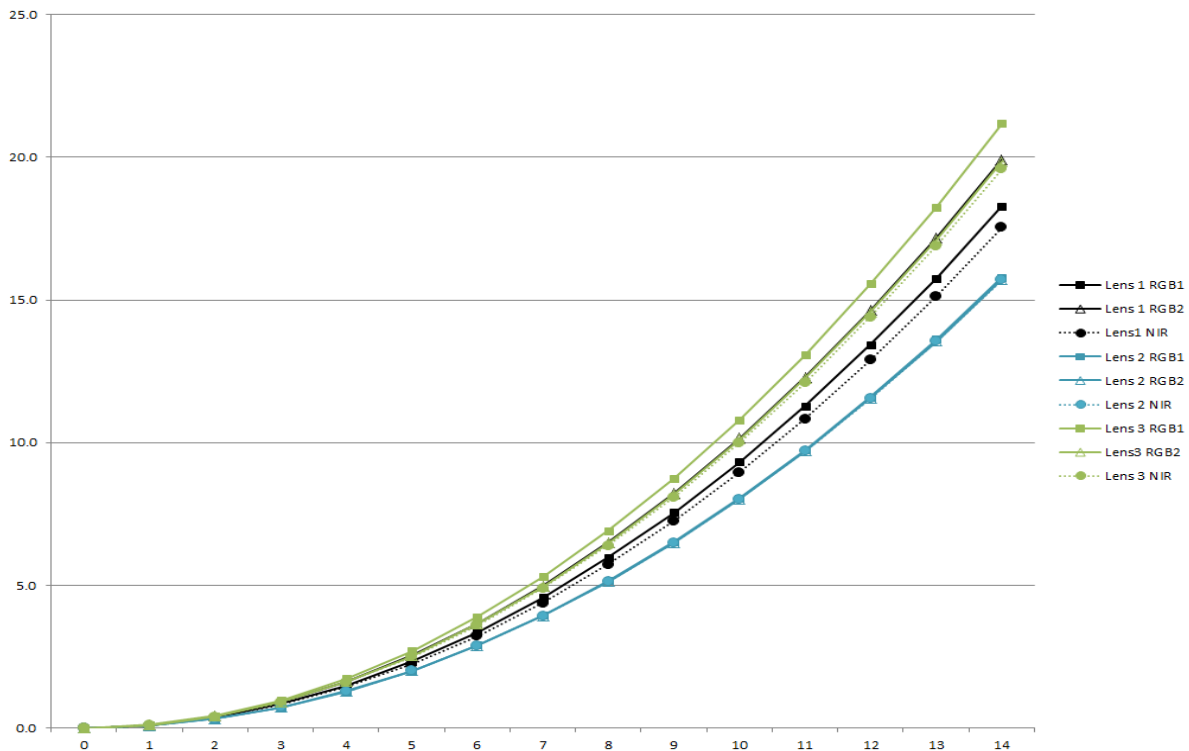


Figure 4. Decentering distortion profiles for the nine combinations of camera and lens. The three profiles for lens 2 are coincident. The profiles for Lens 1 RGB2, Lens 3 RGB2 and Lens 3 NIR are closely aligned.

For the radial distortion, the clustering is more evident at the furthest radial distance from the principal point. However this is in an area of sparse data and a confident conclusion cannot be drawn, despite the fact that the differences in the profiles are significant. For example, at a radius of 10mm, the average precision of the radial lens distortion profile is approximately ± 1 micrometre at a 95% confidence interval, yet there are variations of up to 20 micrometres for the same lens on different cameras.

Table 3 details the relative angle of the maximum profile of decentering distortion (Fryer, 1996) for the nine combinations. This is effectively the orientation of the pattern of decentering distortion. Because decentering distortion is a function of the misalignment of the lens elements, it would be expected that these angles are consistent for each lens, and this is clearly evident in the table.

Lens	Camera		
	RGB1	RGB2	NIR
1	47.3	46.8	46.6
2	28.4	26.9	24.4
3	72.7	72.3	71.3

Table 3. Comparison of decentering lens distortion maximum profile orientation.

The magnitudes of affinity and orthogonality at a radius of 10mm from the principal point are shown in Table 4. For each camera and lens, the amount of variability is indicated by the standard deviation of the values for each column and row, respectively. Across all three cameras, the affinity parameter appears to have the same variability as across the three lenses. However there is a similarity in the values for the two visible light sensitive cameras, whereas the values for the NIR camera follow a different trend. This suggests that, similar to the conclusion drawn by Fraser et al. (1995), the affinity term may be compensating for an optical distortion in the lens, but in this case the spectral sensitivity of the NIR lens changes the magnitude of the effect.

Affinity at 10mm Radius (um)

Lens	Camera			SD
	RGB1	RGB2	NIR	
1	-2.2	-2.7	-0.4	1.2
2	-0.7	-1.1	0.9	1.0
3	-2.6	-2.9	-1.0	1.0
SD	1.0	1.0	1.0	

Orthogonality at 10mm Radius (um)

Lens	Camera			SD
	RGB1	RGB2	NIR	
1	-1.1	-1.5	-1.3	0.2
2	-0.2	-0.6	-1.0	0.4
3	-0.2	-0.5	-0.4	0.1
SD	0.5	0.6	0.5	

Table 4. Comparison of Affinity and Orthogonality for the nine combinations of camera and lens.
SD = standard deviation.

There is no clear trend for the orthogonality, or image shear, parameter across the three cameras or the three lenses. Whilst the standard deviations of the parameters tend to suggest the effect is associated with the lens, the differences in the variability are not substantial. As noted previously, individual parameters are significant, typically an order of magnitude larger than the estimated precision.

Conclusions

This investigation of a multi-camera, multi-lens calibration of the Sony Alpha NEX 5 camera demonstrates that some parameters in the standard calibration set are clearly associated with the physical source. The principal distance of each of the lenses is consistent for all cameras. Some aspects of the distortion profiles of each of the lenses are consistent for all cameras, whilst others are more variable, possibly influenced by the instability of the camera bodies and lens mounts. From this analysis there is inconclusive evidence regarding the principal point, so for the NEX 5 camera the location may be influenced by both the position of the image sensor within the camera body and the position of the optical axis of the lens with respect to the lens mount.

There is some evidence in the results, as previous research has identified, that the affinity term in the camera calibration is associated with an optical signal from the lenses, rather than some physical aspect of the image sensor. However this conclusion is tentative because the NIR camera does not conform to this trend. There is no significant pattern associated with cameras or lenses for the orthogonality parameter. Whilst there is a significant effect, the magnitude is variable and the physical source is unknown.

There is considerable scope for further research into multi-camera, multi-lens calibration of the current generation of digital cameras. A limitation of the research described in this paper is that the cameras and lenses are virtually identical. A clearer trend for the association of calibration parameters with cameras or lenses should be obtained if the cameras and interchangeable lenses are significantly different, as was the case for Fraser et al. (1995) and Shortis et al. (1995). Further, more definitive results should be obtained if cameras with a more reliable body and lens mount are used, in order to minimise the confounding factor of poor stability.

The outcome for the Sony Alpha NEX 5 cameras is mixed. The results of the calibrations clearly indicate that there is variability across the camera and lens combinations, so each combination must be subject to an individual calibration.

The lack of consistency of the results is most likely caused by lack of stability of the camera and lens, which brings into question the reliability of the camera. Nevertheless, the image space precision of approximately one ninth of a pixel is typical for this type of camera and corresponds to a few centimetres on the ground. When combined with the utility and features of the NEX 5, the camera will provide a very effective imaging system for the landscape monitoring.

Acknowledgement

The author gratefully acknowledges the assistance of Dr. Alex Lechner, Centre for Mined Land Rehabilitation, Sustainable Minerals Institute, The University of Queensland, for the considerable time and effort required to provide advice on the cameras, to identify, design and prepare the test field, and then to capture the images for the calibration networks.

References

- Brown, D. C. 1966. Decentring distortion of lenses. *Photogrammetric Engineering*, 22:444-462.
- Brown, D. C., 1971. Close range camera calibration. *Photogrammetric Engineering*, 37(8): 855-866.
- Chikatsu, H. and Takahashi, Y., 2009. Comparative evaluation between consumer grade cameras and mobile phone cameras for close range photogrammetry. *Videometrics, Range Imaging and Applications X*, F. Remondino, M. R. Shortis and S. F. El-Hakim (Eds.), SPIE Vol. 7447, paper 74470H. The International Society for Optical Engineering, Bellingham WA, USA.
- Cramer, M., 2004. EuroSDR network on digital camera calibration. *International Archives of Photogrammetry, Remote Sensing and Spatial Information Sciences*, XXXV-B6, pp. 204-209.
- Faig, W., and Shih, T.-Y., 1988. Functional review of additional parameters. Proceedings, Technical Papers Volume 3, *ACSM-ASPRS Annual Convention*, St. Louis, U.S.A., pp 158-168.
- Fraser, C. S., Digital camera self-calibration, 1997. *ISPRS Journal of Photogrammetry and Remote Sensing*, 52(4): 149-59.
- Fraser, C. S., Shortis, M. R. and Ganci, G., 1995. Multi-sensor system self-calibration. *Videometrics IV*, S. F. El-Hakim (Ed.), SPIE Vol. 2598, pp 2-18. The International Society for Optical Engineering, Bellingham WA, USA. ISBN 0819419621.
- Fraser, C. S., Woods, A., and Brizzi, D., 2005. Hyper redundancy for accuracy enhancement in automated close range photogrammetry. *The Photogrammetric Record*, 20(111): 205-17.
- Fryer, J. G. 1996. Camera calibration. In *Close Range Photogrammetry and Machine Vision*. K. B. Atkinson (ed.). Caithness, United Kingdom: Whittles Publishing, pp 156-179.
- Granshaw, S. I. 1980. Bundle adjustment methods in engineering photogrammetry. *The Photogrammetric Record*, 10(56):181-207.
- Kenefick, J. F., Gyer, M. S. and Harp, B. F. 1972. Analytical self-calibration. *Photogrammetric Engineering and Remote Sensing*, 38(11): 1117-1126.
- Lechner, A.M., A. Fletcher, K. Johansen, and P. Erskine, 2012. Characterising upland swamps using object-based classification methods and hyper-spatial resolution imagery derived from an Unmanned Aerial Vehicle. *ISPRS Annals of Photogrammetry, Remote Sensing and Spatial Information Science*, I-4, 101-106.
- Mills, J. P., Schneider, D., Barber, D. M. and Bryan, P. G., 2003. Geometric assessment of the Kodak DCS Pro Back. *The Photogrammetric Record*, 18(103): 193-208.
- Moniwa, H., 1981. The concept of "photo-variant" self-calibration and its application in block adjustment with bundles. *Photogrammetria* 36(1): 11-29.
- Rieke-Zapp, D. H., 2010. Digital medium-format camera for metric applications - Alpa 12 Metric. *The Photogrammetric Record*, 25(131): 283-298.
- Rieke-Zapp, D., Tecklenburg, W., Peipe, J., Hastedt, H., and Haig, C., 2009. Evaluation of the geometric stability and the accuracy potential of digital cameras – Comparing mechanical stabilization versus parameterisation. *ISPRS Journal of Photogrammetry and Remote Sensing*, 64(3): 248-258.

- Remondino, F. and Fraser, C. S., 2006. Digital camera calibration methods: considerations and comparisons. *International Archives of Photogrammetry, Remote Sensing and Spatial Information Sciences*, Vol. XXXVI, Part 5, pp. 266-272.
- Reulke, R., 2006. Combination of distance data with high resolution images. *International Archives of Photogrammetry, Remote Sensing and Spatial Information Sciences*, Vol. XXXVI, Part 5, 5 pages.
- Shortis, M. R., 2011. Comparisons of calibrations for still image and movie modes for consumer digital cameras. Proceedings on CD-ROM, *GSR_1 Geospatial Science Research Symposium*, RMIT University, December 12-14, paper 30, 11 pages. ISBN 478-0-9872527-0-8.
- Shortis, M. R., Bellman, C. J., Robson, S, Johnston, G. J. and Johnson G. W., 2006. Stability of zoom and fixed lenses used with digital SLR cameras. *International Archives of Photogrammetry and Remote Sensing*, 36(5): 285-290.
- Shortis, M. R. and Beyer, H. A. 1996. Sensor technology for close range photogrammetry and machine vision. In *Close Range Photogrammetry and Machine Vision*. K.B. Atkinson (ed.). Caithness, United Kingdom: Whittles Publishing, 106-155.
- Shortis, M. R., Robson, S. and Beyer, H. A., 1998. Principal point behaviour and calibration parameter models for Kodak DCS cameras. *The Photogrammetric Record*, 16(92): 165-186.
- Shortis, M. R., Snow, W. L. and Goad, W. K., 1995. Comparative geometric tests of industrial and scientific CCD cameras using plumb line and test range calibrations. *ISPRS Intercommission Workshop "From Pixels to Sequences"*, Zurich, Switzerland, pp 53-59.
- Strecha, C., A. Fletcher, A. Lechner, and P. Erskine, 2012. Developing species specific vegetation maps using multi-spectral hyperspatial imagery from unmanned aerial vehicles. *ISPRS Annals of Photogrammetry, Remote Sensing and Spatial Information Science*, I-3, 311-316.
- Wendt, A., and Dold, C., 2005. Estimation of interior orientation and eccentricity parameters of a hybrid imaging and laser scanning sensor. *International Archives of Photogrammetry, Remote Sensing and Spatial Information Sciences*, XXXVI-5/W8, 7 pages.
- Ziemann, H. and El-Hakim, S. F. 1983. On the definition of lens distortion reference data with odd-powered polynomials. *Canadian Surveyor*, 37(3): 135-143.